Received: 1 November 2020 | Revised: 7 December 2020 | Accepted: 18 December 2020

DOI: 10.1002/agt2.18

Aggregate Open Access WILEY

REVIEW

# Self-assembled magnetic nanomaterials: Versatile theranostics nanoplatforms for cancer

**Shuren Wang** | **Zhiyi Wang** | **Yanglong Hou**

Beijing Key Laboratory of Magnetoelectric Materials and Devices Department of Materials Science and Engineering, College of Engineering, Beijing Innovation Centre for Engineering Science and Advanced Technology, Peking University, Beijing, China

**Correspondence**
Prof. Y. Hou, Beijing Key Laboratory of Magnetoelectric Materials and Devices Department of Materials Science and Engineering, College of Engineering, Beijing Innovation Centre for Engineering Science and Advanced Technology, Peking University, Beijing 100871, China.
Email: hou@pku.edu.cn

Authors Shuren Wang, Zhiyi Wang contributed equally.

**Funding information**
Natural Science Foundation of Beijing Municipality, Grant/Award Number: L72008; National Natural Science Foundation of China, Grant/Award Numbers: 51672010, 81421004, 51631001

**Abstract**
Self-assembled magnetic nanomaterials (MNMs) are a class of promising biomaterials possessing excellent physiochemical and biological characteristics, making them highly attractive in biomedical applications. A myriad of magnetic nanosystems can be created by using self-assembly as a synthetic tool. Favorable nano-bio interfacial properties are shown in these promising self-assembled magnetic nanosystems, while still retaining their physical/chemical functionalities. This review aims to provide a systematical overview of the self-assembled MNMs. In addition, this review highlights their implementations in cancer theranostics in detail. Overall, this review points out the direction for the application of self-assembled MNMs in biomedicine, and presents how clinical oncology could benefit from the self-assembled nanotechnology.

**KEYWORDS**
biomedicine, cancer theranostics, self-assembled magnetic nanomaterials, self-assembled nanotechnology

## 1 | INTRODUCTION

Due to the serious limitation of drug resistance in conventional pharmaceuticals,[1,2] new avenues for the theranostics of cancers have been provided by the expansion of nanotechnology.[3–7] Thanks to their controllable size, morphology, and physio-chemical properties, pharmaceutical nanoagents have shown great potential in solving healthcare-related cancer issues.[8–10] Nanomaterials with pharmaceutical properties could be prepared by using many kinds of materials, including liposomes, polymers, biomacromolecules, and many other inorganic nanomaterials.[2,5,11–20] In addition, the activity of these nanomaterials can be adjusted and improved by surface modification,[2,10,21] which will promote their in-depth study in biomedicine. The development of many advanced nanosystems in biomedicine have been inspired by these interesting properties. In particular, nanoplatforms with these nanostructures fabricated by self-assembled strategies have demonstrated extensive advantages during the laboratory and preclinical studies for theranostics of cancer.[22–25]

The most significant feature of the self-assembly process is based on the energy minimization trend from disordered state to ordered state, and it is a strategy different from covalent conjugation,[13,26–30] which depends on some relatively weak noncovalent interactions, including hydrogen bonding, van der Waals, electrostatic interaction, and hydrophobic interaction.[28,30–32] There are many examples of self-assembled nanomaterials according to this classification, including DNA, proteins, lipid vesicles, and superlattice nanocrystals.[18,26,27,33,34] The self-assembly process can be realized by the external magnetic fields. Magnetic nanomaterials (MNMs) for biomedical applications constructed by self-assembly nanotechnology can comprehensively utilize the inherent properties of each basic assembly unit. The scientific progress in MNMs by self-assembly and their

**Abbreviations:** $\beta$-CD, $\beta$-cyclodextrin; 1D, one-dimensional; 2D, two-dimensional; 3D, three-dimensional; AMF, alternating magnetic field; AuNWs, gold nanowreaths; *b*-MNP-PGEA, polycation-functionalized bowl-shaped magnetic assembly; Ce6, chlorin e6; cRGDyK, acyclic Arg-Gly-Asp; DDSs, drug delivery systems; ES-MIONs, exceedingly small magnetic iron oxide NPs; FDA, Food and Drug Administration; Gd, gadolinium; GdIO, Gd-embedded iron oxide; GSH, glutathione; HSA, human serum albumin; MHT, magnetic hyperthermia therapy; MNMs, magnetic nanomaterials; MNPs, Magnetic nanoparticles; MRI, magnetic resonance imaging; NPs, nanoparticles; NSMs, iron oxide NPs shelled microbubbles; PDT, photodynamic therapy; PEI, polyethylenimine; PTT, photothermal therapy; PTX, paclitaxel; SAMNs, self-assembled into magnetic nanoclusters; SPIONs, superparamagnetic iron oxide NPs; TEM, Transmission electron microscope; USPIO, ultra-small superparamagnetic iron oxide; UV, ultraviolet

This is an open access article under the terms of the Creative Commons Attribution License, which permits use, distribution and reproduction in any medium, provided the original work is properly cited.
© 2021 The Authors. *Aggregate* published by South China University of Technology; AIE Institute and John Wiley & Sons Australia, Ltd.

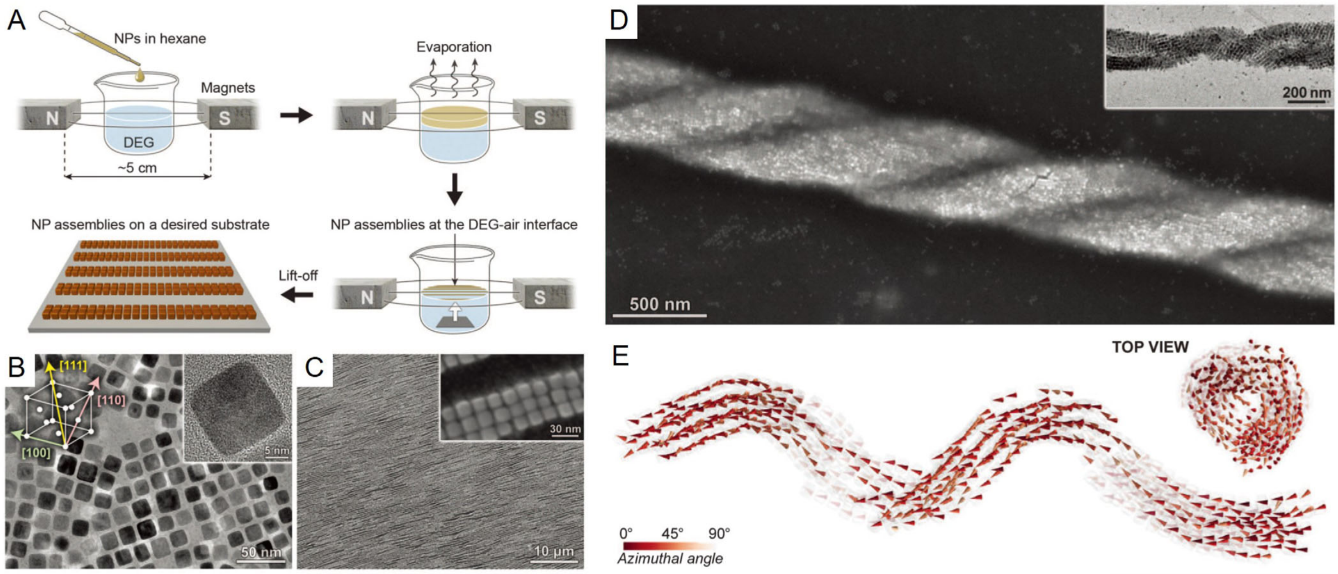


**FIGURE 1** Magnetic field induced self-assembly. (A) In the schematic diagram of the experimental setup, the hexane solution evaporates under the external magnetic field; (B) transmission electron microscope (TEM) image of $Fe_3O_4$ rounded nanocubes as assembly units; (C) scanning electron microscope (SEM) images of belts$_{100}$; (D) SEM and TEM images of double helix; (E) imaging from Monte Carlo simulations of 1D belt folding into a helix. Reproduced with permission.[39] Copyright 2014 American Association for the Advancement of Science

potential applications in cancer theranostics are reviewed by us according to the current critical studies. First, the construction strategies of self-assembled MNMs are briefly discussed to prove people's interest in self-assembled MNMs in this review. Subsequently, we focus on the integration of biomedical diagnosis system, including $T_1$-weighted magnetic resonance imaging (MRI), $T_2$-weighted MRI, and $T_1/T_2$ dual-mode MRI. Furthermore, the imaging-guided treatment systems are also reviewed, including drug delivery systems (DDSs), photothermal therapy (PTT), photodynamic therapy (PDT), and magnetic hyperthermia therapy (MHT). Above all, we highlight the advantages and existing challenges in potential clinical application for self-assembled MNMs, which will be beneficial to increase the investment in science and technology.

## 2 | CONSTRUCTION OF SELF-ASSEMBLED MNMs

### 2.1 | Magnetic field–induced self-assembly

Magnetic field is a significant means to study the magnetic properties of materials. Magnetic field has been developed as a new condition for the synthesis and assembly of MNMs with the development of self-assembly, which is similar to traditional reaction conditions (for instance, reaction time, temperature). So far, magnetic fields have been widely used for nanomaterials assembled of one-dimensional (1D), two-dimensional (2D), and three-dimensional (3D) aggregates.[30,35–37] As well known, most MNMs exhibit anisotropy. The so-called easy magnetic axis is the direction that can lead to minimization of the energy of the magnetization vector for single-phase nanocrystalline ferromagnets. The easy magnetic axis of $Fe_3O_4$ is along the [111] and [110] directions. Therefore, the formation of 1D MNM can be prepared by a well-controlled external magnetic field along the easy magnetic axis. Wang et al. reported growth of $Fe_3O_4$ nanowires induced by the magnetic field.[38] Subsequently, Taheri et al. reported the discovery of an interesting magnetic field–induced self-assembled phenomenon of cubic nanoparticles (NPs) in solution (Figures 1(A)–1(E)).[39] The interaction between the induced magnetic dipole and the external field was very weak, which was on the order of van der Waals force. The past decades have witnessed the progress of the self-assembly of MNMs under magnetic fields. Interestingly, important effects on magnetic domain, crystal structure, and product phase are shown by the applied magnetic field during chemical synthesis. It is easier to prepare materials with higher magnetic susceptibility due to the enhancement of magnetic exchange coupling in the reaction system under the external magnetic field. In addition, the magnetic field also shows their great ability in NPs' assembly. Magnetic field–induced self-assembly simplifies the operation steps, but requires accurate magnetic field control equipment to achieve, which increases the dependence on the equipment.

### 2.2 | Magnetic nanoparticles (MNPs)-based self-assembly

MNPs-based self-assembly is a kind of self-assembly of hard particles.[28,40,41] The predicting of the self-assembled superlattices can be obtained by comparing the relative stabilities of candidate structures. It is necessary to estimate the free energy by approximate method due to the difficulty of considering all the energy contribution in the system. The hard particle model is very suitable for this study to provide a good approximation method to describe nanocrystals with major repulsion or weak attraction in a short distance. For instance, 10 kinds of binary nanocrystal superlattices with both 2D and 3D order, through control of the core size of nanospheres and the molecular weight, were reported by Ye et al. (Figures 2(A)–2(F)).[32] As claimed by the authors, these results provided new opportunities for creating mechanically robust inorganic–organic materials with

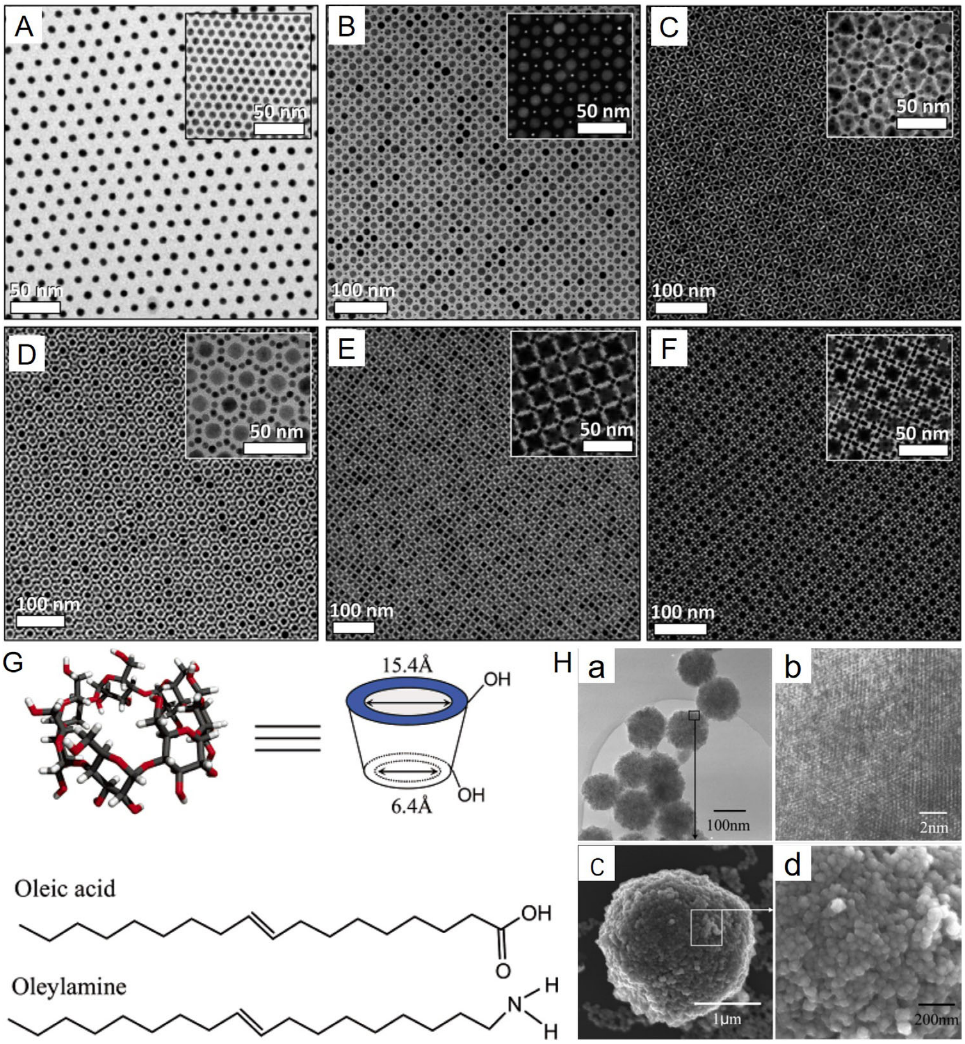


**FIGURE 2** MNPs-based self-assembly. (A) TEM image of Au NPs capped with polystyrene (PS). The same NPs cores without treatment is at inset; (B) TEM image of PS-capped Au and $Fe_3O_4$ NPs. Dark-field STEM image of the same NPs is at inset. TEM images of (C) $MgZn_2$, (D) $CaCu_5$, (E) $C_{60}K_6$, and (F) $NaZn_{13}$ comprised of PS-capped Au and $Fe_3O_4$ NPs. Reproduced with permission.[32] Copyright 2015 Nature Publishing Group. (G) Chemical structures of $\beta$-CD and oleic acid, and oleylamine; (H) TEM (a and b) and SEM images (c and d) of sample B. Reproduced with permission.[30] Copyright 2005 American Chemical Society Publishing Group

controllable nanoscale interfaces and microstructures. Moreover, Hou et al. reported an approach to assemble MNPs into 3D nanospheres by organic phase syntheses with surfactants including $\beta$-cyclodextrin ($\beta$-CD), oleic acid, and oleylamine (Figures 2(G) and 2(H)).[30] This approach could be used for the assembling process of other MNPs such as Ni NPs, Co NPs, and $Fe_3O_4$ NPs. Such self-assembly strategy might play an important role in the construction of DDSs. However, the self-assembly based on MNPs requires high-quality NPs, so the expansion of the system will be limited.

## 2.3 | DNA–MNPs self-assembly

DNA is considered as a core genetic biological molecule in living systems. Although DNA molecules are composed of simple units, different deoxynucleotide chains and flexible conformations can be achieved through precise design and organization, which can be programmed. In other words, this is the nature of DNA self-assembly. For example, Ma et al. introduced DNA-modified MNPs, Y-scaffolds, and DNA linkers into the framework of DNA hydrogels to construct magnetic controllable DNA hydrogels.[42] It was noteworthy that the chemical covalent bond between MNPs surface amino group and DNA terminal sulfhydryl group could improve the stability of hybrid DNA–MNPs hydrogel. Furthermore, the DNA–MNPs hydrogel can get various stimuli such as temperature, enzyme, and magnetic field during the gel-to-sol transition. Wang et al. designed a titanium dioxide ($TiO_2$)-coated magnetite microspheres–DNA dendrimers biological complex as a signal amplifier for electrochemical detection of polynucleotide kinase activity.[43] As the peroxidase-like activity of MNPs could catalyze the reduction of hydrogen peroxide, the synergistic effect among MNPs, $TiO_2$, and DNA dendrimers produced significant electrochemical signals, which could be used to detect the activity of polynucleotide kinases sensitively. Despite all this, the development of DNA–MNPs self-assembly is limited by the activity of DNA, which may be influenced in the existence of MNPs.

## 2.4 | Molecular switches–based self-assembly

Molecular switches, such as azobenzene, pyrrolidine, and dithiophenene, are another important family of

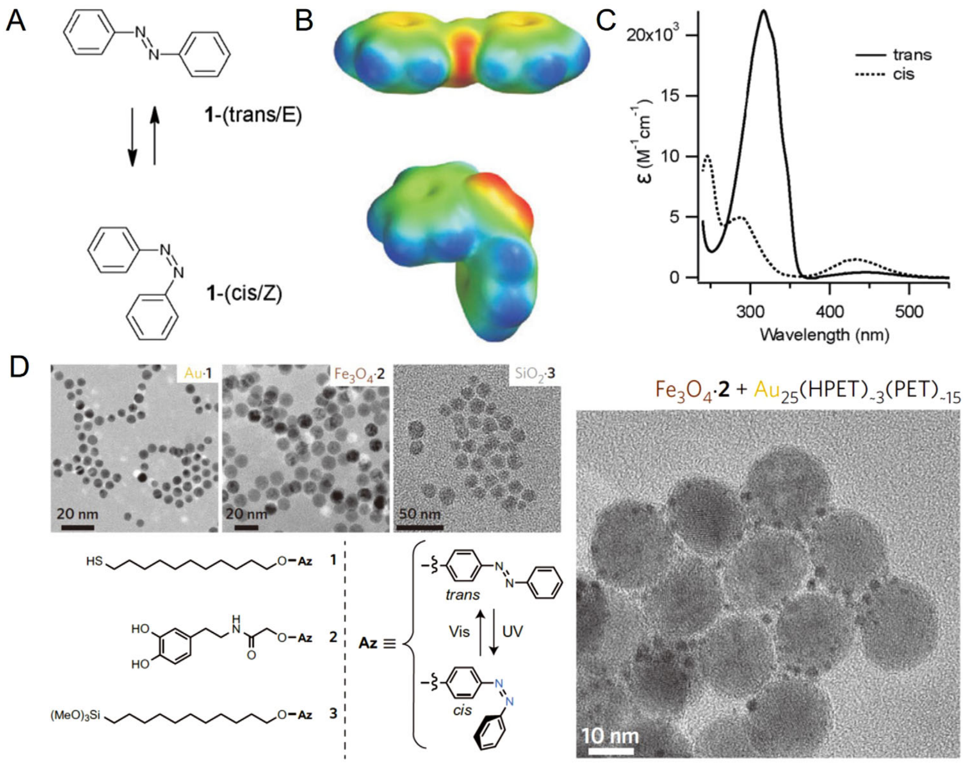


**FIGURE 3** Molecular switches-based self-assembly. (A) Lewis structure of the azobenzene photoisomerization process; (B) calculated electron density maps for trans- and cis-azobenzene isomers with calculated electron density maps; (C) electronic absorption spectra of the trans- and cis-azobenzene dissolved in ethanol. Reproduced with permission.[46] Copyright 2011 The Royal Society of Chemistry Publishing Group. (D) TEM imaging and construction strategy diagram of photoresponsive Au NPs, $Fe_3O_4$ NPs, $SiO_2$ NPs, and obtained self-assembly $Fe_3O_4$-$Au_{25}$ by irradiation of switch-functionalized NPs. Reproduced with permission.[47] Copyright 2016 Nature Publishing Group

**TABLE 1** Current self-assembled magnetic nanomaterials and their typical applications and representative references

| Self-assembled structure | Self-assembly unit | Assembly technique | Application | Reference |
|---|---|---|---|---|
| $Fe_3O_4$-QDs nanocomposite | $Fe_3O_4$ NPs and CdTe QDs | Cross-linked method | Magnetic resonance imaging (MRI) and Multicolor fluorescent imaging | Ref. 48 |
| Magnetic janus amphiphilic NPs | Co cluster-embedded $Fe_3O_4$ NPs | Ultrasonication-triggered self-assembly approach | Cancer theranostic | Ref. 49 |
| Hydrophobic magnetic NP-encapsulated amphiphilic polysaccharide-clasped self-assembly | $Fe_3O_4$ NPs | Electrohydrodynamic spraying | MRI | Ref. 50 |
| Magnetic hydrogel | $Fe_3O_4$ nanospheres | Magnetic field-directed assembly | Enhancement of magnetothermal effect | Ref. 51 |
| Magnetic nanoparticle chains | Co NPs | Magnetic flow coating | Sensors | Ref. 52 |

unconventional ligands for guiding the self-assembly of nanocrystals.[26,44,45] Molecular switches are expected to realize the reversible remote control of the aggregation behavior of nanocrystals by light-induced structural isomerization. For example, azobenzene in trans isomers became cis under ultraviolet (UV) irradiation (Figure 3(A)). The cis state was slowly converted back to trans at room temperature, which could be accelerated by thermal or blue light (Figure 3(B)). When the other end of azobenzene was modified and could tether with the binding group on the surface of nanocrystalline, their binding to the surface of nanocrystalline could trigger the assembly and recrystallization of nanocrystalline remotely. However, under UV irradiation, the dipole–dipole interaction between terminal cis-azobenzene groups promoted the mixing of ligand crown ethers, resulting in the precipitation of nanocrystals from the solution (Figure 3(C)).[46] It was worth noting that this photoinduced instability process could proceed very gently to form regular polyhedral superlattices. This was further confirmed by the self-assembly $Fe_3O_4$-$Au_{25}$ nanostructures reported by *Zhao et al*. (Figure 3(D)).[47] Therefore, the molecular switches–based self-assembly can be used as a universal assembly strategy, which is worth further development in the future.

To sum up, these self-assembly strategies reported above provide a variety of choices for the preparation of MNMs. In recent years, the important research progress from assembling MNMs is shown in Table 1. It can be seen from the Table 1 that the synthesis strategies and applications of self-assembled MNMs have become diversified. However, the clinical transformation of self-assembled MNMs in

biomedicine is still facing great challenges. More sustained scientific research in this field is needed in the future.

# 3 | BIOMEDICAL APPLICATIONS OF SELF-ASSEMBLED MNPs

## 3.1 | Diagnostic systems

Imaging techniques are indispensable tools to provide biological information in cancer diagnosis and therapy, especially at the cellular and molecular levels in living systems. Self-assembled MNPs have been proved to have high efficiency in ameliorating the navigation of diagnostic agents to the target sites and combining several diagnostic moieties in relatively simple delivery system. In this section, the advance of self-assembled MNPs in common medical diagnostic modalities, principally about MRI, will be reviewed.

MRI is a kind of noninvasive imaging technique, which makes full use of the corresponding spin properties of different nuclei to conduct morphological and functional imaging in a magnetic field, with high resolution generation of many tissues such as brain, muscles, and tumors.[53] In clinics, MRI has the irreplaceability with the advantages of high image contrast, high spatial resolution, and no ionizing radiation. In recent years, resolution improvement even at the single cell level has been the trend in MRI research field. Taken into consideration that ordinary materials-mediated MRI has lower sensitivity to targeted molecules expressed on the cancer cells, special targeted contrast agents or probes are required in MRI detecting processes. Self-assembly NPs have the extensive application potential in targeted diagnosis due to their ability of controlled surface modification. In addition to paramagnetic materials, including superparamagnetic iron oxide NPs (SPIONs) and gadolinium (Gd) chelates, some magnetic isotopes of other elements such as $^{13}C$, $^{31}P$, $^{19}F$, and $^{23}Na$, have also served as contrast agents of MRI.[54] In general, two kinds of timing parameters such as longitudinal ($T_1$) and transverse ($T_2$) relaxation time weighting are most constantly employed for MRI contrast enhancement between the pathological and normal tissues owing to the intrinsic low sensitivity of MRI.[16]

### 3.1.1 | $T_1$-weighted MRI

Gd-based $T_1$ contrast agents are usually used for the purpose of reducing the spin-lattice relaxation times of vicinity water, to make the targeted area "brighter" in $T_1$-weighted MRI. As a new kind of MR contrast agent, Gd-based NPs in the self-assembly way were developed with Acetyl-Arg-Val-Arg-Arg-Cys(StBu)-Lys(Gd-DOTA)-CBT, which was susceptive to furin, a kind of tumor-overexpressed protease. Intracellular glutathione (GSH) induced the fracture of disulfide bond of the Cys motif and subsequently furin also cleaved RVRR motif of the NP precursors, with the generation of active intermediate, which condensed to yield the amphiphilic dimers with a hydrophobic macrocyclic core for self-assembled Gd-based NPs via $\pi$–$\pi$ stacking interaction. The relaxivity of the formed dimers was significantly enhanced in contrast to NP precursors, which suggested that the self-assembly Gd-based NPs exerted more advantageous MRI performance. Meanwhile, the intracellular self-assembly Gd-based NPs also enhanced MR contrast in the furin-overexpressed MDA-MB-468 cells *in vivo*.[55] Subsequently, an interesting study revealed that the different binding sites of $Gd^{3+}$ with different building blocks of NPs precursors induced otherness on the magnetic relaxivity of the complexes. For example, $Mo_2O_4(OAc)$ and $Mo_2O_4(HPO_4{}^{2-})$ moieties improved $Gd^{3+}$-bound keplerates-mediated $T_1$ and $T_2$ relaxivity values, however, this process was restricted on account of that the free keplerates were degraded rapidly in aqueous solutions. Hence, to enhance the stability, the keplerate complexes were self-assembled into ultra-small NPs with hydrophilic coating by a triblock copolymer. The optimal keplerate compositions had the performance of low cytotoxicity and high stability, furthermore, with the superior $T_1$ and $T_2$ relaxivity values (95 and 114 $mM^{-1}$ $s^{-1}$, accordingly) for MRI.[56] In addition to $Gd^{3+}$, other self-assembled NPs also served as MRI agents. Magnetic gold nanowreaths (AuNWs) were synthesized in layer-by-layer self-assembled way, which were responsive to GSH. Silica was skillfully designed as the layer between AuNW as the inner core and exceedingly small magnetic iron oxide NPs (ES-MIONs) as the outside shell, which were composed into the magnetic AuNW (Figure 4(A)). Thereinto, the nanostructures such as Au branches, small junctions, and central holes improved photothermal properties of magnetic AuNM compared to Au nanorings via strong plasmon coupling. In terms of imaging, the assembled ES-MIONs were released from magnetic AuNWs through GSH-induced response, leading to enhance the $T_1$ imaging ability. In detail, the GSH solution enhanced the longitudinal relaxivity of magnetic AuNWs at 2.8 times compared to that before incubation *in vitro* and the tumor microenvironment increased the imaging effects of magnetic AuNWs within tumor accumulation at 2.5 times through $T_1$ imaging signal compared to the individual ES-MIONs *in vivo* (Figure 4(B)), which further suggested that GSH with the high concentration in tumor microenvironment was the intelligent switch that turned on the magnetic AuNWs-mediated $T_1$ imaging signal (Figure 4(C)). Meanwhile, the intensive photoacoustic effect of magnetic AuNWs exerted the effective photoablation of tumors in imaging-guided PTT (Figure 4(D)).[57]

### 3.1.2 | $T_2$-weighted MRI

Usually, owing to a blood system that has the faster clearance on the ultra-small superparamagnetic iron oxide (USPIO) NPs, they predictably show weaker magnetic resonance properties of $T_2$ imaging signal than large MNPs or aggregates. Hence, to synthetize, the MNPs with appropriate size and excellent MR properties are of great importance in the field of imaging. Iron-based NPs exhibit incomparable advantages over other magnetic NPs.[12,58] Magnetic Hägg iron carbide NPs ($Fe_5C_2$ NPs) were synthesized with carbon shell coating and showed the high-saturation magnetization nature that made $Fe_5C_2$ NPs as an excellent candidate for $T_2$ MRI contrast agents (Figure 5(A)). The *in vivo* results indicated the lowest imaging signal of $T_2$-weighted MRI for 24 h postinjection, revealing it as the optimal time for tumor theranostics (Figure 5(B)).[9] Interestingly, the assembly of iron carbide NPs and other NPs have expanded their application potential in the field of MRI. Iron carbide ($Fe_5C_2@Fe_3O_4$) NPs in

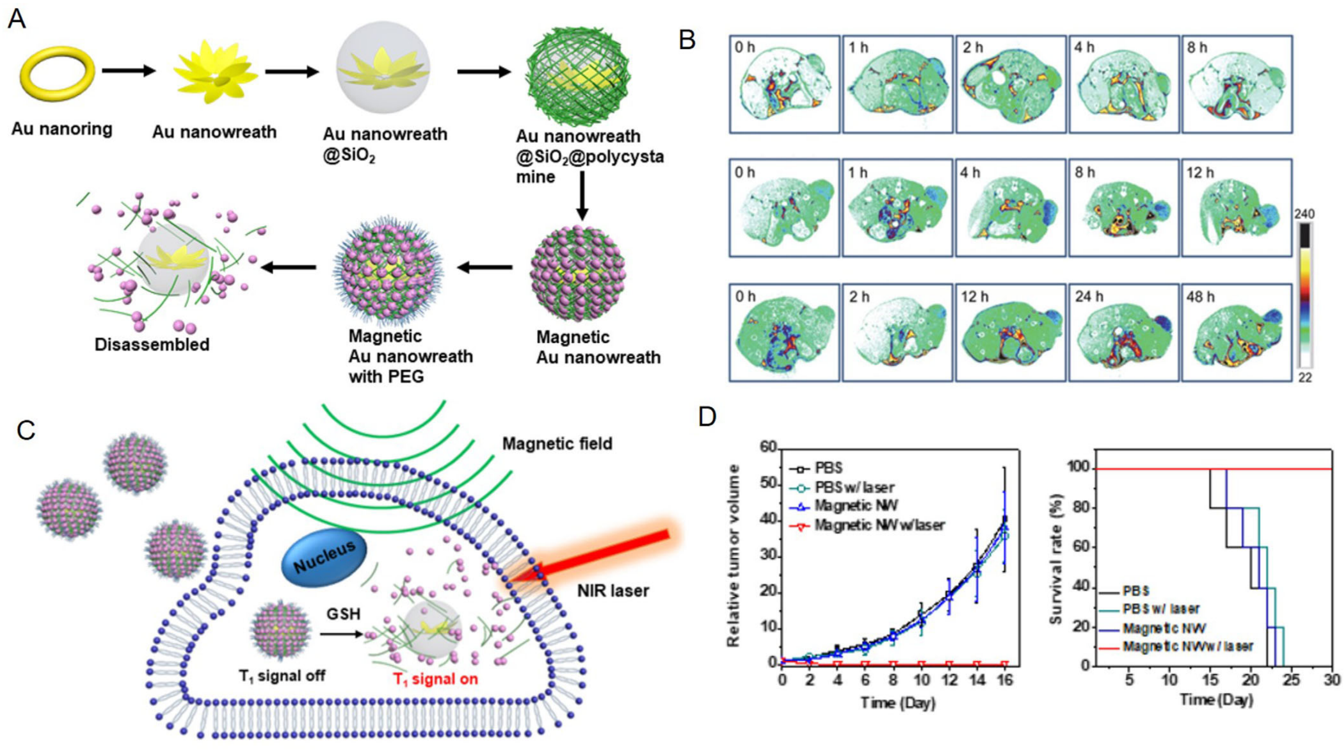


**FIGURE 4** GSH-responsive self-assembled AuNWs enhanced MRI and imaging-guided PTT. (A) Schematic illustration of the synthesis of magnetic AuNWs; (B) $T_1$-weighted MR images of U87MG tumor-bearing nude mice at different timepoints after the injection of AuNWs into mice; (C) schematic illustration of the mechanism of that AuNWs turned on the $T_1$-weighted MRI signals through GSH in tumor microenvironment; (D) relative tumor volume and survival curves of the treated mice and other controlled mice. Reproduced with permission.[57] Copyright 2018 American Chemical Society

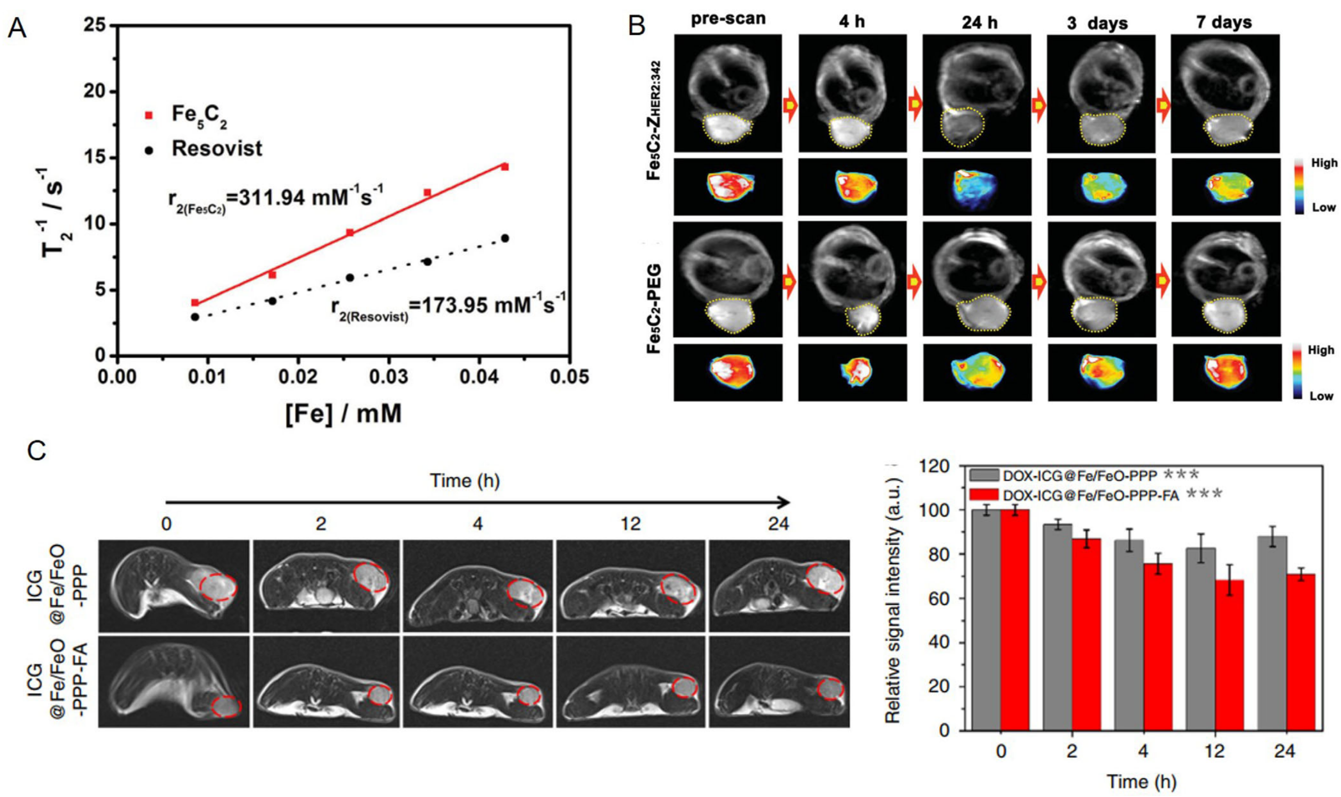


**FIGURE 5** Iron-based NPs exhibited excellent $T_2$-weighted MRI signal. (A) $T_2$ relaxation rate ($1/T_2$) of the $Fe_5C_2$ NPs and Resovist; (B) $T_2$-weighted MR images of tumor-bearing mice with the injection of $Fe_5C_2$ NPs. Reproduced with permission.[9] Copyright 2014 WILEY-VCH Verlag GmbH & Co. KGaA, Weinheim. (C) Real-time MRI of tumor-bearing mice and the relative MRI signal intensities changing at the tumor site with injection of NPs. Reproduced with permission.[10] Copyright 2019 Nature Publishing Group

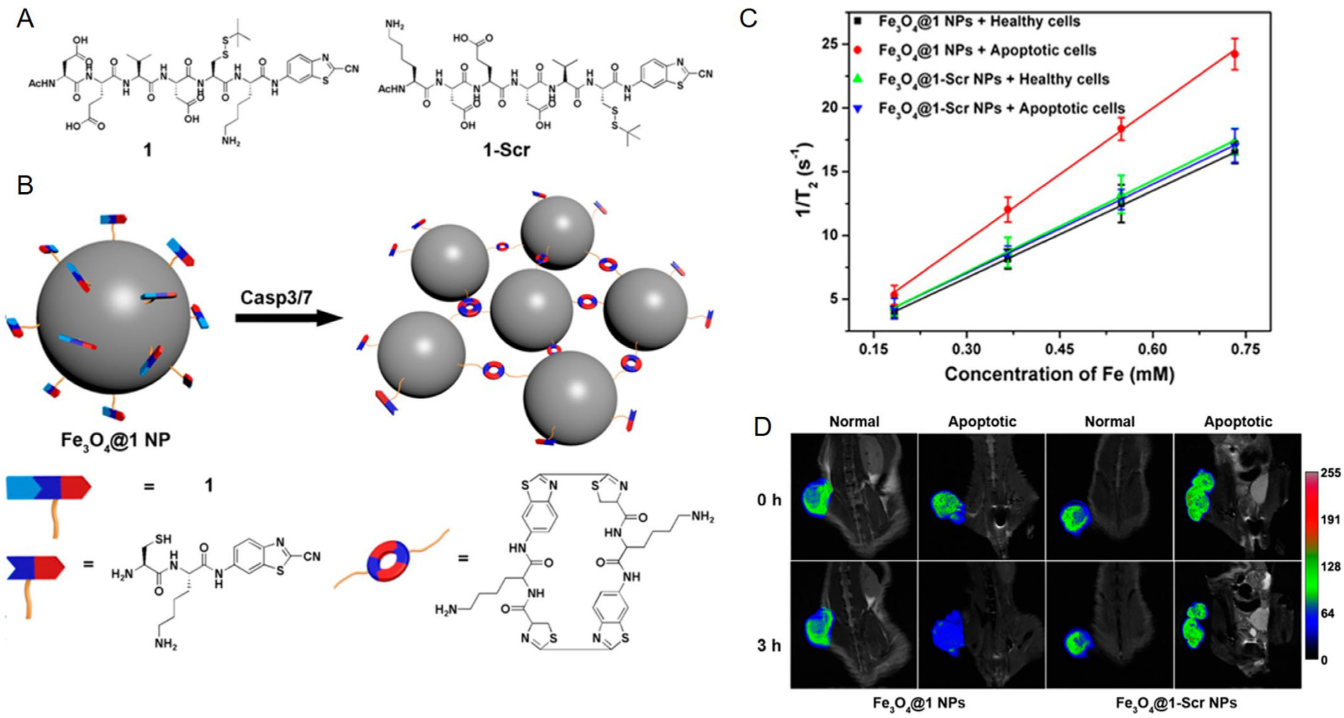


**FIGURE 6** Intracellular self-assembly of $Fe_3O_4$ NPs trigged by enzymes improved $T_2$-weighted MRI of cancer cell apoptosis. (A) The structures of 1 and 1-Scr; (B) schematic illustration of the aggregation of $Fe_3O_4$@1 NPs induced by Cas3/7; (C) $T_2$ relaxation rates ($1/T_2$) of $Fe_3O_4$@1 NPs or $Fe_3O_4$@1-Scr NPs with different concentrations in the healthy or apoptotic HepG2 cells; (D) *In vivo* $T_2$-weighted MRI of treated mice and other control mice. Reproduced with permission.[59] Copyright 2016 American Chemical Society

the core-shell structure[17] and monodisperse Au-$Fe_2C$ Janus NPs[18] exhibited enhanced $T_2$ imaging signal in tumor sites whether were modified with active targeting molecules on the surface. Moreover, Fe/FeO core-shell nanocrystals also had the $T_2$-weighted MRI capability. The imaging of Figure 5(C) clearly showed the strong signal intensity and made the tumor dark, with the higher sensitivity to targeted molecules.[10] On the other hand, intracellular aggregation or self-assembly of USPIO NPs is also usually considered as an optimized strategy for $T_2$-weighted MRI. A kind of Ac-Asp-Glu-Val-Asp-Cys (StBu)-Lys-CBT–modified USPIO NPs based on $Fe_3O_4$ for $T_2$-weighted MRI were designed through the enzyme-promoted condensation reaction (Figure 6(A)). The NP precursors were subjected to GSH reduction and Caspase 3-cleavage to yield the cyclized dimers, subsequently, led to self-assembly of individual $Fe_3O_4$ NPs into larger MNPs (Figure 6(B)). The *in vitro* (Figure 6(C)) and *in vivo* (Figure 6(D)) results indicated that self-assembled $Fe_3O_4$ NPs–enhanced $T_2$ imaging signal mediated by tumor apoptosis.[59]

### 3.1.3 | $T_1/T_2$ dual-mode MRI

Some paramagnetic materials used as T1 contrast agents, represented by $Gd^{3+}$ chelates, can generate a bright contrast with high signal intensity, but are limited due to their insensitivity and low MR relaxivity.[60] Alternatively, $T_2$ contrast agents such as SPION, are comparatively sensitive to the detection of pathological tissue, while have low signal-to-noise ratios induced by the artifacts and dark contrast.[61] Consequentially, MR contrast agents with the advantages of $T_1$ and $T_2$ contrast are recommendable for superior MRI. These dual-mode contrast agents simultaneously provide the capacity of the contrast and sensitivity enhancement through signal reconstruction and visualization.[62] Recent investigations into $T_1/T_2$ dual-mode contrast agents have evolved to the single self-assembled MNPs consisting of $T_1$ and $T_2$ contrast agents.[63] A new smart $T_1/T_2$ dual-mode contrast agent was successfully fabricated by the targeted CD105 peptide CL 1555, amphiphilic block copolymer PEG-*b*-poly (ε-caprolactone) as the shell, and dozens of hydrophobic $MnFe_2O_4$ MNPs as the core. The designed nanostructure in self-assembled fashion had the higher relaxivity than single $MnFe_2O_4$ MNPs. Initially, the complex NPs mediated $T_2$-weighted MRI for the CL 1555 labeled tumor vascular endothelial cells in the dark contrast. Subsequently, the $Mn^{2+}$ ions were released from $MnFe_2O_4$ MNPs, with the results of making the $T_1$-weighted MRI signal intensity enhanced, which provided a novel nanoprobe for $T_1$- and $T_2$-dual mode MRI of tumor angiogenesis.[64] Another kind of $T_1$- and $T_2$-dual mode MRI-visible vector was self-assembled into nanoclusters with a core of Gd-embedded iron oxide (GdIO) NPs and a shell of stearic acid-modified low molecular weight polyethylenimine (PEI). By forming nanoaggregates, the NPs exerted the enhanced $r_2$ value compared to the GdIO-DMSA NPs through the strong exchange coupling effect, while the similar $r_1$ value to that of GdIO-DMSA NPs through a strong integration effect. This smart nanoplatform provided the new strategy of noninvasive $T_1$- and $T_2$-dual mode MRI monitoring capability.[65]

## 3.2 | Imaging-guided therapeutic systems

Imaging-guided therapeutic systems are the crucial tools to achieve visual and accurate treatment in cancer therapy.[66] Self-assembled MNPs as DDSs can transport therapeutic agents to targeted sites *in vivo* through functionalizing

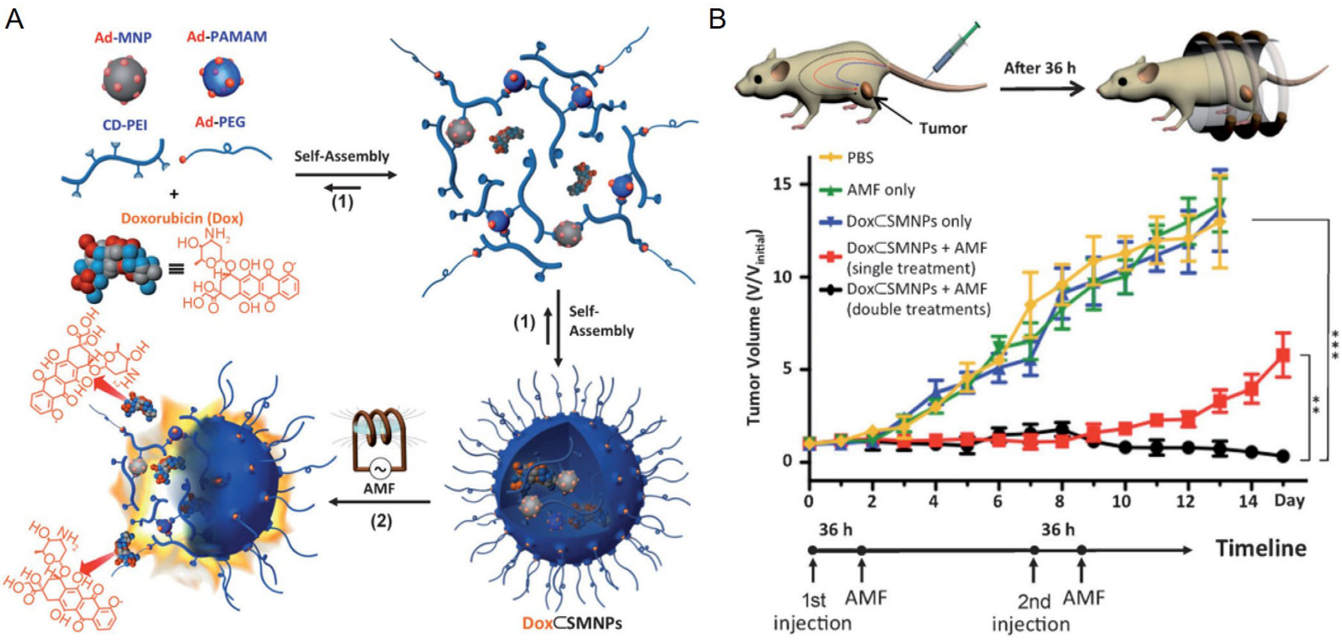


**FIGURE 7** Self-assembled MNPs as the drug release system for *in vivo* cancer treatment. (A) Schematic illustration of molecular design, self-assembly, and function of magnetothermally responsive DoxSMNPs; (B) treatment scheme of DoxSMNPs in mice and the tumor volume of the treated mice and other controlled mice. Reproduced with permission.[69] Copyright 2013 Wiley-VCH Verlag GmbH & Co. KGaA, Weinheim

the surface, in order to improve the treatment efficiency. On the other hand, self-assembled MNPs also have some intrinsic properties to trigger PTT and PDT. In this section, the advance of self-assembled magnetic NPs-mediated imaging-guided therapeutic systems in cancer therapy will be reviewed.

### 3.2.1 | DDSs

Chemotherapeutic drugs are usually effective in tumor inhibition,[67,68] however, due to the pervasive toxicity, the safe and efficient DDSs are urgently needed. A kind of MNPs as DDSs was designed in the self-assembled synthetic strategy. Doxorubicin (Dox)-encapsulated supramolecular MNPs (DoxSMNPs) was made from a fluorescent anticancer drug Dox and four molecular building blocks: Ad-PAMAM, 6 nm Ad grafted $Zn_{0.4}Fe_{2.6}O_4$ superparamagnetic NP (Ad-MNP), CD-PEI, and Ad-polyethylene glycol (PEG) (Figure 7(A)). The self-assembled MNPs were triggered in the heat transformer to lead to the burst release of Dox in alternative magnetic field, with the results of significant inhibition effect on tumors (Figure 7(B)), which suggested that this drug delivery/release system with temporal and spatial controllability as drug candidates may increase selectivity and reduce side effects of drugs with higher toxicity.[69] SPIONs have been approved to be applied in cancer imaging, diagnostics, and treatment by the Food and Drug Administration (FDA) due to their excellent biocompatibility. A kind of SPIO NPs that self-assembled into magnetic nanoclusters (SAMNs) were developed as a theranostic nanosystem. PEG and paclitaxel (PTX) were maintained through high affinity complexation in the $\beta$-CD cavity that conjugated to SPIO NPs. Interestingly, in addition to that large cluster size and dense iron oxide core enhanced MR contrast, a special peptide targeting to the tumors made SAMNs accumulated into tumors in abundance, which made the signal of tumor more distinct. PTX loaded into $\beta$-CD was released in a controlled manner with the results of more accurate and efficient treatment effect.[70] Similarly, the four-arm PEG-poly(e-caprolactone) copolymers were designed to form a kind of magnetic star-shaped micelles in the self-assembled way with disulfide bonds as intermediate linkers. Antitumor chemotherapy drug Dox and magnetic iron oxide NPs ($Fe_3O_4$) were loaded into the hydrophobic cores. The NPs were effectively transported to the tumor in a dual-targeted way with the salic acid–mediated active targeting and magnetic field–mediated passive targeting, leading to a high therapeutic efficacy to tumor cells.[71] Excepted for DDSs, self-assembled MNPs were also designed to deliver some DNAs for gene therapy. Magnetic $Fe_3O_4$ NPs were self-assembled in the form of a polycation-functionalized bowl-shaped magnetic assembly (*b*-MNP-PGEA). MNP-PGEA was incorporated with some cationic polymer, which achieved the pDNA condensation via electrostatic interactions. The *in vivo* results indicated that the combination therapy with $Fe_3O_4$ NPs-mediated PTT and gene therapy showed stronger tumor inhibition effect than monotherapy.[72]

### 3.2.2 | PTT

PTT is an important tumor ablation treatment, which makes the conversion from light energy to heat by laser irradiation.[11,73] Hence, the strategy of PTT and chemotherapy has attracted much attention of research in cancer therapy. Recently, Chen group reported a Pt prodrug polyphenol and $Gd^{3+}$-loaded cancer theranostics nanoplatform containing a mild acidic pH and thermal sensitive polymer for multimodal therapy (Figure 8(A)). PEG–PDI–PDPA polymer and PEG–PDI-$C_{20}$ were self-assembled to form the appropriate cores and shells. Pt prodrug polyphenols chelated with $Gd^{3+}$ (3%) were encapsulated in the core with high loading efficiency of drug (20%). The self-assembled NPs were trigged to

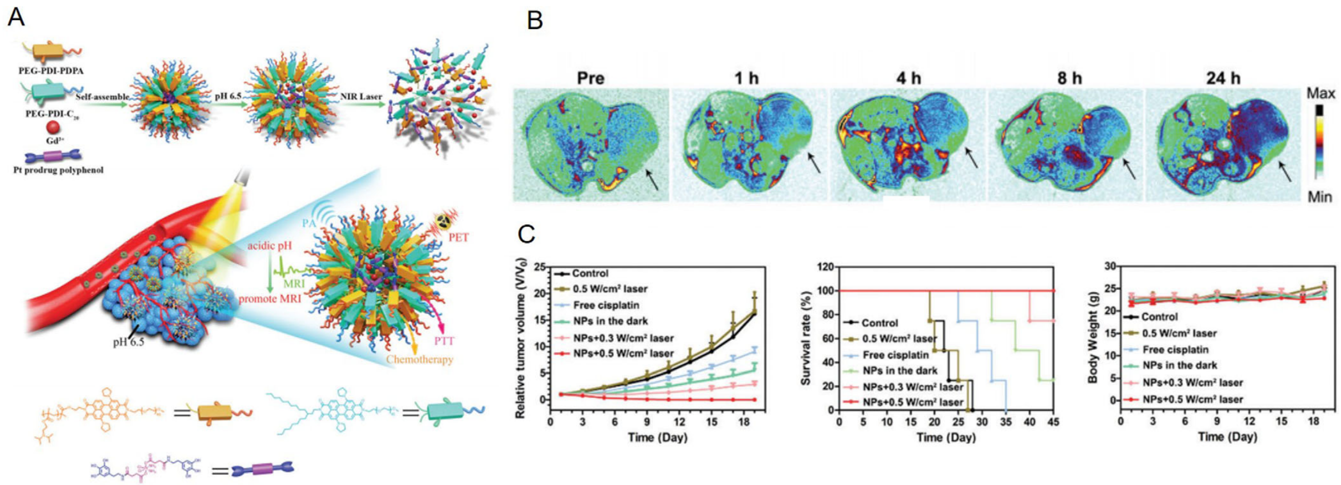


**FIGURE 8** Self-assembled MNPs as tumor microenvironment-responsive nanotheranostics for cancer therapy. (A) Schematic illustration of the formulation and mechanism of the NPs for cancer theranostics; (B) *in vivo* $T_1$-weighted MRI of U87MG tumor-bearing mice after intravenous injection of GPDPA NPs for 1, 4, 8, and 24 h; (C) the relative tumor volume curves and survival curve and body weight of the mice with different treatments. Reproduced with permission.[74] Copyright 2019 The Royal Society of Chemistry

heat generated by external NIR irradiation and tumor-specific acidic pH to release Pt drug in the controlled manner, which reduced the side effects of Pt drug to normal tissues. In terms of imaging, the signal of MR was increased at three folds in $T_1$ relaxivity, which provided real-time tracking of NPs for combination therapy (Figure 8(B)). Of course, the animal results showed the significant inhibition effect on tumor in the synergistic therapy combining PTT and chemotherapy (Figure 8(C)).[74] Moreover, self-assembled iron oxide NPs shelled microbubbles (NSMs) were fabricated in one nanotherapeutic platform with the multiple synergizing responsiveness (e.g., magnetism, acoustics, and optics). NSMs could be targeted to the tumor site in magnetic field in a passive way. Subsequently, iron oxide NPs were released triggered by ultrasound, with the results of facilitating the penetration of NPs deep into the tumor due to the cavitation effect of microbubbles. Magnetic hyperthermia and PTT mediated by iron oxide NPs inhibited the growth of different tumors to overcome drug resistance due to the heterogeneity of tumors, which exerted a promising combined treatment of tumors.[75]

### 3.2.3 | PDT

PDT is a novel cancer therapy containing three elements, including oxygen, light, and a photosensitizer, leading to reactive oxygen species generation, which is lethal to cancer cells.[76] PDT has many advantages over conventional cancer therapies such as minimal invasiveness, low systemic toxicity, and high response. Liu group designed a kind of drug-induced self-assembly of modified albumins as nano-theranostics nanoplatform. Abraxane as an FDA-approved nanomedicine drug was provided with the antitumor effect through the mechanism of that PTX could bind to human serum albumin (HSA) via hydrophobic interaction. According to the strategy, the self-assembly of HSA modified with either a photosensitizer chlorin e6 (Ce6) or acyclic Arg-Gly-Asp (cRGDyK) peptide was induced by PTX. Ce6 provided the chelating site for $Mn^{2+}$ to mediate MRI. On the other hand, cRGDyK peptides induced active targeting R$v\beta$3-integrin overexpressed on tumor angiogenic endothelium. Both two kinds of albumin-based NPs exhibited obviously improved therapeutic efficacy on tumors in the combination with PDT and chemotherapy. This work provided a new designed strategy of self-assembly method trigged by drug for multiscale imaging-guided cancer therapy.[77] Different self-assembly strategies of MNPs were also used in the PDT of cancer. The fabrication of a supramolecular nanoplatform via the amphiphilic amino acid (9-fluorenylmethyloxycarbonyl-L-leucine, Fmoc-L-L)-modulated self-assembly of an MRI contrast agent (ionic manganese, $Mn^{2+}$) and photosensitive drug (chlorin e6, Ce6) were designed. Fmoc-L-L, Ce6, and $Mn^{2+}$ actuated self-assembly coordination bonds with a nanoscale supramolecular network via hydrophobic interaction and $\pi$-stacking. This kind of NPs had the capability of high drug loading, intrinsic good biocompatibility, and stability. More importantly, the NPs were reactive to GSH that was at the high concentration in the tumor microenvironment, which trigged the disassembly of NPs. Photosensitizer-trigged PDT was used to enhance tumor ablation in the cooperative assembly process of these components with the synchronization effect, and to improve the reductive tumor microenvironment via the competitive coordination of GSH with $Mn^{2+}$, which suggested a self-assembly of a multifunctional theranostic nanoplatform from minimalist biological building blocks.[78]

### 3.2.4 | MHT

MHT is the approach that utilizes the heat generation of MNPs in the external alternating magnetic field (AMF) to achieve the therapeutic effects. MHT has been attempted to diversified cancers including lung, breast, prostate, and liver cancers.[79] Multifunctional theranostic nanoplatforms were designed with superparamagnetic $Fe_3O_4$ NPs and photoluminescent PbS/CdS quantum dots in the self-assembled way. Interestingly, this kind of self-assembled MNPs had the dual capacity of magnetothermal therapy and PTT, which were more efficient than single thermal therapy for cancer treatment. The results indicated that the dual thermal energy transfer efficiency had seven times amplification compared with magnetic heating alone.[80] Another kind of

SPION-loaded nanocapsule hydrogels were also developed for MHT. The nanostructure consisted of self-assembled poly(organophosphazene) nanocapsules as the shell and embedded SPIONs as the core. Multiple MHT induced the cancer cell death via necrosis and showed no damage to the healthy tissues around tumors, which greatly improved the efficiency of MHT than single magnetic thermal ablation.[81]

In conclusion, self-assembled MNPs for constructing multifunctional materials have opened the prospects of biomedical application in translational fields with the advantages of relatively simple preparation, high stability, multivalent effect, and potential clinical translation value. Interestingly, a kind of self-assembled of magnetic and photoluminescent NPs were developed for disease detection *in vitro*. Iron oxide NPs modified with antibodies to capture targeted proteins performed the function of magnetic enrichment and manganese-doped zinc sulfide (ZnS:Mn) NPs as photoluminescent substrate were used for quantitative measurement of protein. This sandwich assay format provided with the advantages of dispensing with washing steps and enhancing the cascade amplification of signal. Simultaneously, this kind of self-assembled NPs effectively increased the detection sensitivity and economized the cost of enzyme-linked immunosorbent assay, which improved the potential of clinical disease *in vitro* detection.[82] Although most of present research have focused on the basic research, *in vivo* experiments can still provide some theoretical guidance for clinical translation, including diagnosis and treatment. In order to give impetus to the clinical application of self-assembled MNPs, the biocompatibility *in vivo* should be considered. Some surface modification through organic molecules has provided biocompatibility and long-term stability of self-assembled MNPs *in vitro*.[83] On the other hand, the cell toxicity effect of self-assembled MNPs is closely bound up with the concentration of MNPs. In general, high dose of NPs may be more likely to induce cell growth inhibition. While most cells can survive under a low concentration of MNPs due to the relatively high colloidal stability, even a small amount of quantum dots are retained *in vivo*.[84] Although biocompatibility has been improved by concentration control,[84] surface modification,[85] and electric charge change,[86] it is still the direction of further optimization in the future. It is worth mentioning that appropriated size and surface modification can allow self-assembled MNPs to be metabolized out through the kidney and liver, leading to further reduce toxicity *in vivo*.[87]

## 4 | CONCLUSIONS AND OUTLOOK

In conclusion, self-assembly technology can develop MNMs with good structure and biological activity, which are very suitable for biomedical applications. These self-assembled magnetic nanostructures can be easily and efficiently combined with a large number of biological functional agents, so they can be customized according to specific needs. So far, their high potential applications have been proved by several successful examples. However, as discussed in the previous section, although these nanosystems envision a bright future for us, these findings do not immediately benefit cancer patients by translating them into clinical practice. The structure–function correlation and potential molecular mechanism need to be further revealed, which may be the key to enhance its effective application in biomedicine. Nevertheless, we believe that with the development of nanotechnology and biotechnology, these obstacles will eventually be overcome, and the application of self-assembled magnetic nanosystems may be extended to more healthcare fields in the future.

## ACKNOWLEDGMENTS

This work was financially supported by the Natural Science Foundation of Beijing Municipality (L72008) and the National Natural Science Foundation of China (51672010, 81421004, 51631001).

## CONFLICT OF INTEREST

The authors declare no conflict of interest.

## ORCID

*Yanglong Hou* https://orcid.org/0000-0003-0579-4594

## REFERENCES

1. A. V. Biankin, S. Piantadosi, S. J. Hollingsworth, *Nature* **2015**, *526*, 361.
2. J. Yu, Y. M. Ju, L. Y. Zhao, X. Chu, W. L. Yang, Y. L. Tian, F. G. Sheng, J. Lin, F. Liu, Y. H. Dong, Y. L. Hou, *ACS Nano* **2016**, *10*, 159.
3. Y. M. Ju, B. Dong, J. Yu, Y. L. Hou, *Nano Today* **2019**, *26*, 108.
4. R. Hao, R. Xing, Z. Xu, Y. Hou, S. Gao, S. Sun, *Adv. Mater.* **2010**, *22*, 2729.
5. K. Zhu, Y. M. Ju, J. J. Xu, Z. Y. Yang, S. Gao, Y. L. Hou, *Acc. Chem. Res.* **2018**, *51*, 404.
6. T. Danino, A. Prindle, G. A. Kwong, M. Skalak, H. Li, K. Allen, J. Hasty, S. N. Bhatia, *Sci. Transl. Med.* **2015**, *7*, 289ra84.
7. L. Wu, X. Qu, *Chem. Soc. Rev.* **2015**, *44*, 2963.
8. A. Wicki, D. Witzigmann, V. Balasubramanian, J. Huwyler, *J. Controlled Release* **2015**, *200*, 138.
9. J. Yu, C. Yang, J. D. S. Li, Y. C. Ding, L. Zhang, M. Z. Yousaf, J. Lin, R. Pang, L. B. Wei, L. L. Xu, F. G. Sheng, C. H. Li, G. J. Li, L. Y. Zhao, Y. L. Hou, *Adv. Mater.* **2014**, *26*, 4114.
10. Z. Wang, Y. Ju, Z. Ali, H. Yin, F. Sheng, J. Lin, B. Wang, Y. Hou, *Nat. Commun.* **2019**, *10*, 4418.
11. Z. Wang, Y. Ju, S. Tong, H. Zhang, J. Lin, B. Wang, Y. Hou, *Nanoscale Horiz.* **2018**, *3*, 624.
12. J. Yu, F. Chen, W. Gao, Y. Ju, X. Chu, S. Che, F. Sheng, Y. Hou, *Nanoscale Horiz.* **2017**, *2*, 81.
13. F. Liu, Y. J. Jin, H. B. Liao, L. Cai, M. P. Tong, Y. L. Hou, *J. Mater. Chem. A* **2013**, *1*, 805.
14. S. Mura, D. T. Bui, P. Couvreur, J. Nicolas, *J. Controlled Release* **2015**, *208*, 25.
15. J. Li, L. T. Mo, C. H. Lu, T. Fu, H. H. Yang, W. H. Tan, *Chem. Soc. Rev.* **2016**, *45*, 1410.
16. Z. Y. Wang, J. Liu, T. R. Li, J. Liu, B. D. Wang, *J. Mater. Chem. B* **2014**, *2*, 4748.
17. J. Yu, F. Zhao, W. L. Gao, X. Yang, Y. M. Ju, L. Y. Zhao, W. S. Guo, J. Xie, X. J. Liang, X. Y. Tao, J. Li, Y. Ying, W. C. Li, J. W. Zheng, L. Qiao, S. B. Xiong, X. Z. Mou, S. L. Che, Y. L. Hou, *ACS Nano* **2019**, *13*, 10002.
18. Y. Ju, H. Zhang, J. Yu, S. Tong, N. Tian, Z. Wang, X. Wang, X. Su, X. Chu, J. Lin, Y. Ding, G. Li, F. Sheng, Y. Hou, *ACS Nano* **2017**, *11*(9), 9239.
19. F. Liu, Y. L. Hou, S. Gao, *Chem. Soc. Rev.* **2014**, *43*, 8098.
20. Z. Y. Wang, J. Hai, T. R. Li, E. L. Ding, J. X. He, B. D. Wang, *ACS Sustain. Chem. Eng.* **2018**, *6*, 9921.
21. W. W. Chen, S. H. Zhang, Y. Y. Yu, H. S. Zhang, Q. J. He, *Adv. Mater.* **2016**, *28*, 8567.
22. Q. Xia, Z. K. Chen, Z. Q. Yu, L. Wang, J. Q. Qu, R. Y. Liu, *ACS Appl. Mater. Inter.* **2018**, *10*, 17081.
23. G. Chen, Y. Yang, Q. Xu, M. Ling, H. Lin, W. Ma, R. Sun, Y. Xu, X. Liu, N. Li, Z. Yu, M. Yu, *Nano Lett.* **2020**, *20*, 8141.
24. Y. F. Xiao, F. F. An, J. X. Chen, J. Yu, W. W. Tao, Z. Yu, R. Ting, C. S. Lee, X. H. Zhang, *Small* **2019**, *15*.

25. Y. Yang, Y. Yu, H. Chen, X. Meng, W. Ma, M. Yu, Z. Li, C. Li, H. Liu, X. Zhang, H. Xiao, Z. Yu, *ACS Nano* **2020**, *14*, 13536.
26. M. A. Boles, M. Engel, D. V. Talapin, *Chem. Rev.* **2016**, *116*, 11220.
27. Y. H. Dong, C. Yao, Y. Zhu, L. Yang, D. Luo, D. Y. Yang, *Chem. Rev.* **2020**, *120*, 9420.
28. L. H. Zhang, J. J. Wu, H. B. Liao, Y. L. Hou, S. Gao, *Chem. Commun.* **2009**, 4378.
29. C. Yang, J. J. Wu, Y. L. Hou, *Chem. Commun.* **2011**, *47*, 5130.
30. Y. Hou, H. Kondoh, M. Shimojo, E. O. Sako, N. Ozaki, T. Kogure, T. Ohta, *J. Phys. Chem. B* **2005**, *109*, 4845.
31. S. Y. Qin, A. Q. Zhang, S. X. Cheng, L. Rong, X. Z. Zhang, *Biomaterials* **2017**, *112*, 234.
32. X. C. Ye, C. H. Zhu, P. Ercius, S. N. Raja, B. He, M. R. Jones, M. R. Hauwiller, Y. Liu, T. Xu, A. P. Alivisatos, *Nat. Commun.* **2015**, 6.
33. J. Yu, X. Chu, Y. L. Hou, *Chem. Commun.* **2014**, *50*, 11614.
34. G. B. Qi, Y. J. Gao, L. Wang, H. Wang, *Adv. Mater.* **2018**, *30*.
35. L. Hu, R. R. Zhang, Q. W. Chen, *Nanoscale* **2014**, *6*, 14064.
36. M. S. Wang, L. He, Y. D. Yin, *Mater. Today* **2013**, *16*, 110.
37. Z. Y. Yang, T. S. Zhao, X. X. Huang, X. Chu, T. Y. Tang, Y. M. Ju, Q. Wang, Y. L. Hou, S. Gao, *Chemical Science* **2017**, *8*, 473.
38. J. Wang, Q. W. Chen, C. Zeng, B. Y. Hou, *Adv. Mater.* **2004**, *16*, 137.
39. G. Singh, H. Chan, A. Baskin, E. Gelman, N. Repnin, P. Kral, R. Klajn, *Science* **2014**, *345*, 1149.
40. C. Yang, H. Zhao, Y. Hou, D. Ma, *J. Am. Chem. Soc.* **2012**, *134*, 15814.
41. J. J. Wu, J. H. Zhu, M. G. Zhou, Y. L. Hou, S. Gao, *Crystengcomm* **2012**, *14*, 7572.
42. J. Q. Zhuang, H. M. Wu, Y. A. Yang, Y. C. Cao, *J. Am. Chem. Soc.* **2007**, *129*, 14166.
43. G. F. Wang, L. Chen, X. P. He, Y. H. Zhu, X. J. Zhang, *Analyst* **2014**, *139*, 3895.
44. R. Klajn, J. F. Stoddart, B. A. Grzybowski, *Chem. Soc. Rev.* **2010**, *39*, 2203.
45. R. Klajn, *Chem. Soc. Rev.* **2014**, *43*, 148.
46. A. A. Beharry, G. A. Woolley, *Chem. Soc. Rev.* **2011**, *40*, 4422.
47. H. Zhao, S. Sen, T. Udayabhaskararao, M. Sawczyk, K. Kucanda, D. Manna, P. K. Kundu, J. W. Lee, P. Kral, R. Klajn, *Nat. Nanotechnol.* **2016**, *11*, 82.
48. J. Li, J. Zhang, Z. Guo, H. Jiang, H. Zhang, X. Wang, *Langmuir* **2020**, *36*, 14471.
49. X. L. Liu, M. L. Peng, G. L. Li, Y. Q. Miao, H. Luo, G. Y. Jing, Y. He, C. Zhang, F. Zhang, H. M. Fan, *Nano Lett.* **2019**, *19*, 4118.
50. J. C. Park, D. Kim, Y. H. Song, H. J. Cha, J. H. Seo, *ACS Appl. Mater. Inter.* **2020**, *12*, 38899.
51. K. Hu, J. F. Sun, Z. B. Guo, P. Wang, Q. Chen, M. Ma, N. Gu, *Adv. Mater.* **2015**, *27*, 2507.
52. H. Y. Yuan, I. J. Zvonkina, A. M. Al-Enizi, A. A. Elzatahry, J. Pyun, A. Karim, *ACS Appl. Mater. Inter.* **2017**, *9*, 11290.
53. E. Terreno, D. D. Castelli, A. Viale, S. Aime, *Chem. Rev.* **2010**, *110*, 3019.
54. Z. Zhou, Z. R. Lu, *Adv. Drug Del. Rev.* **2017**, *113*, 24.
55. C. Y. Cao, Y. Y. Shen, J. D. Wang, L. Li, G. L. Liang, *Sci. Rep.* **2013**, *3*, 1024.
56. J. Elistratova, B. Akhmadeev, V. Korenev, M. Sokolov, I. Nizameev, A. Gubaidullin, A. Voloshina, A. Mustafina, *Soft Matter* **2018**, *14*, 7916.
57. Y. J. Liu, Z. Yang, X. L. Huang, G. C. Yu, S. Wang, Z. J. Zhou, Z. Y. Shen, W. P. Fan, Y. Liu, M. Davisson, H. Kalish, G. Niu, Z. H. Nie, X. Y. Chen, *ACS Nano* **2018**, *12*, 8129.
58. J. Xu, K. Zhu, Y. Hou, *ACS Appl. Mater. Inter.* **2020**, *12*, 36811.
59. Y. Yuan, Z. L. Ding, J. C. Qian, J. Zhang, J. Y. Xu, X. J. Dong, T. Han, S. C. Ge, Y. F. Luo, Y. W. Wang, K. Zhong, G. L. Liang, *Nano Lett.* **2016**, *16*, 2686.
60. M. H. Kim, B. Kim, E. K. Lim, Y. Choi, J. Choi, E. Kim, E. Jang, H. S. Park, J. S. Suh, Y. M. Huh, S. Haam, *Macromol. Biosci.* **2014**, *14*, 943.
61. Z. Zhou, D. Huang, J. Bao, Q. Chen, G. Liu, Z. Chen, X. Chen, J. Gao, *Adv. Mater.* **2012**, *24*, 6223.
62. K. Cheng, M. Yang, R. Zhang, C. Qin, X. Su, Z. Cheng, *ACS Nano* **2014**, *8*, 9884.
63. T. H. Shin, J. S. Choi, S. Yun, I. S. Kim, H. T. Song, Y. Kim, K. I. Park, J. Cheon, *ACS Nano* **2014**, *8*, 3393.
64. M. Gong, H. Yang, S. Zhang, Y. Yang, D. Zhang, Z. Li, L. Zou, *Int. J. Nanomed.* **2016**, *11*, 4051.
65. X. Y. Wang, Z. J. Zhou, Z. Y. Wang, Y. X. Xue, Y. Zeng, J. H. Gao, L. Zhu, X. Z. Zhang, G. Liu, X. Y. Chen, *Nanoscale* **2013**, *5*, 8098.
66. S. Wang, Z. Sun, Y. Hou, *Adv. Healthc. Mater.* **2020**, e2000845.
67. S. Wang, K. Ma, L. Chen, H. Zhu, S. Liang, M. Liu, N. Xu, *Biosci. Rep.* **2016**, *36*, e00386.
68. S. Wang, K. Ma, C. Zhou, Y. Wang, G. Hu, L. Chen, Z. Li, C. Hu, Q. Xu, H. Zhu, M. Liu, N. Xu, *Ther. Adv. Med. Oncol.* **2019**, *11*, 1758835919843736.
69. J. H. Lee, K. J. Chen, S. H. Noh, M. A. Garcia, H. Wang, W. Y. Lin, H. Jeong, B. J. Kong, D. B. Stout, J. Cheon, H. R. Tseng, *Angew. Chem. Int. Ed. Engl.* **2013**, *52*, 4384.
70. D. H. Nguyen, J. S. Lee, J. H. Choi, K. M. Park, Y. Lee, K. D. Park, *Acta Biomater*. **2016**, *35*, 109.
71. Z. M. Tang, L. Zhang, Y. Wang, D. Li, Z. D. Zhong, S. B. Zhou, *Acta Biomater*. **2016**, *42*, 232.
72. R. R. Wang, X. G. Dai, S. Duan, N. N. Zhao, F. J. Xu, *Nanoscale* **2019**, *11*, 16463.
73. J. Nam, S. Son, L. J. Ochyl, R. Kuai, A. Schwendeman, J. J. Moon, *Nat. Commun.* **2018**, *9*, 1074.
74. Z. Yang, Y. L. Dai, L. L. Shan, Z. Y. Shen, Z. T. Wang, B. C. Yung, O. Jacobson, Y. J. Liu, W. Tang, S. Wang, L. S. Lin, G. Niu, P. T. Huang, X. Y. Chen, *Nanoscale Horiz*. **2019**, *4*, 426.
75. Y. Yin, S. Y. Wang, D. N. Hu, J. Y. Cai, F. B. Chen, B. Wang, Y. Gao, *Jove-J. Vis. Exp.* **2020**, *159*, e61208.
76. S. B. Brown, E. A. Brown, I. Walker, *Lancet Oncol*. **2004**, *5*, 497.
77. Q. Chen, X. Wang, C. Wang, L. Z. Feng, Y. G. Li, Z. Liu, *ACS Nano* **2015**, *9*, 5223.
78. H. Zhang, K. Liu, S. K. Li, X. Xin, S. L. Yuan, G. H. Ma, X. H. Yan, *ACS Nano* **2018**, *12*, 8266.
79. K. Mahmoudi, A. Bouras, D. Bozec, R. Ivkov, C. Hadjipanayis, *Int. J. Hyperthermia* **2018**, *34*, 1316.
80. F. Yang, A. Skripka, M. S. Tabatabaei, S. H. Hong, F. Ren, A. Benayas, J. K. Oh, S. Martel, X. Liu, F. Vetrone, D. Ma, *ACS Nano* **2019**, *13*, 408.
81. Z. Q. Zhang, S. C. Song, *Biomaterials* **2016**, *106*, 13.
82. D. Kim, H. J. Kwon, K. Shin, J. Kim, R. E. Yoo, S. H. Choi, M. Soh, T. Kang, S. I. Han, T. Hyeon, *ACS Nano* **2017**, *11*, 8448.
83. S. Klein, M. Kizaloglu, L. Portilla, H. Park, T. Rejek, J. Hummer, K. Meyer, R. Hock, L. V. R. Distel, M. Halik, C. Kryschi, *Small* **2018**, *14*, e1704111.
84. L. Ye, K. T. Yong, L. W. Liu, I. Roy, R. Hu, J. Zhu, H. X. Cai, W. C. Law, J. W. Liu, K. Wang, J. Liu, Y. Q. Liu, Y. Z. Hu, X. H. Zhang, M. T. Swihart, P. N. Prasad, *Nat. Nanotechnol.* **2012**, *7*, 453.
85. C. D. Walkey, J. B. Olsen, H. B. Guo, A. Emili, W. C. W. Chan, *J. Am. Chem. Soc.* **2012**, *134*, 2139.
86. P. Rivera-Gil, D. J. De Aberasturi, V. Wulf, B. Pelaz, P. Del Pino, Y. Y. Zhao, J. M. De La Fuente, I. R. De Larramendi, T. Rojo, X. J. Liang, W. J. Parak, *Acc. Chem. Res.* **2013**, *46*, 743.
87. G. B. Yang, S. Z. F. Phua, A. K. Bindra, Y. L. Zhao, *Adv. Mater.* **2019**, *31*, e1805730.

## AUTHOR BIOGRAPHIES

**Shuren Wang** is a postdoc under supervision of Prof. Yanglong Hou in materials science at Peking University after the postdoctoral training in cancer immunology at Tsinghua University. In 2012, she received her B.S. degree in life science and technology from Sichuan University. In 2017, she received her Ph.D. degree in cancer cell biology from Peking Union Medical College. Her main research interests are the nanoparticles on biological applications, especially cancer diagnosis and therapy.

**Zhiyi Wang** is presently undergoing postdoctoral training under supervision of Prof. Yanglong Hou in materials science at Peking University. He received his B.S. degree in chemistry from Heilongjiang University in 2012 and obtained his Ph.D. degree in inorganic chemistry from Lanzhou University in 2018. His main research interests are the magnetic nanomaterials on biological applications, especially cancer diagnosis and therapy.

**Yanglong Hou** earned his Ph.D. in materials science from Harbin Institute of Technology (China) in 2000. After a short postdoctoral training at Peking University, he worked at the University of Tokyo from 2002 to 2005 as a JSPS foreign special researcher and also at Brown University from 2005 to 2007 as a postdoctoral researcher. He joined Peking University in 2007, and is now a professor of materials science. His research interests include the design and chemical synthesis of functional nanoparticles, and their biomedical and energy-related applications.

**How to cite this article:** Wang S, Wang Z, Hou Y. Self-assembled magnetic nanomaterials: versatile theranostics nanoplatforms for cancer. *Aggregate*. **2021**;*2*:e18. https://doi.org/10.1002/agt2.18